# Homology modeling and docking studies of a Δ9-fatty acid desaturase from a Cold-tolerant Pseudomonas sp. AMS8

**Lawal Garba** [1, 2, 3], **Mohamad Ariff Mohamad Yussoff** [4], **Khairul Bariyyah Abd Halim** [4], **Siti Nor Hasmah Ishak** [1], **Mohd Shukuri Mohamad Ali** [1, 5], **Siti Nurbaya Oslan** [1, 5], **Raja Noor Zaliha Raja Abd. Rahman** Corresp. [1, 2]

[1] Enzyme and Microbial Technology Research Centre, Faculty of Biotechnology and Biomolecular Sciences, Universiti Putra Malaysia, Serdang, Selangor, Malaysia
[2] Department of Microbiology, Faculty of Biotechnology and Biomolecular Sciences, Universiti Putra Malaysia, Serdang, Selangor, Malaysia
[3] Department of Microbiology, Faculty of Science, Gombe State University, Gombe, Gombe state, Nigeria
[4] Department of Biotechnology, Kulliyyah of Science, International Islamic University, Kuantan, Pahang Darul Makmur, Malaysia
[5] Department of Biochemistry, Faculty of Biotechnology and Biomolecular Sciences, Universiti Putra Malaysia, Serdang, Selangor, Malaysia

Corresponding Author: Raja Noor Zaliha Raja Abd. Rahman
Email address: rnzaliha@upm.edu.my

Membrane-bound fatty acid desaturases perform oxygenated desaturation reactions to insert double bonds within fatty acyl chains in regioselective and stereoselective manners. The Δ9-fatty acid desaturase strictly creates the first double bond between C9 and 10 positions of most saturated substrates. As the three-dimensional structures of the bacterial membrane fatty acid desaturases are not available, relevant information about the enzymes are derived from their amino acid sequences, site-directed mutagenesis and domain swapping in similar membrane-bound desaturases. The Cold-tolerant Pseudomonas sp. AMS8 was found to produce high amount of monounsaturated fatty acids at low temperature. Subsequently, an active Δ9-fatty acid desaturase was isolated and functionally expressed in Escherichia coli. In this paper we report homology modeling and docking studies of a Δ9-fatty acid desaturase from a Cold-tolerant Pseudomonas sp. AMS8 for the first time to the best of our knowledge. Three dimensional structure of the enzyme was built using MODELLER version 9.18 using a suitable template. The protein model contained the three conserved-histidine residues typical for all membrane-bound desaturase catalytic activity. The structure was subjected to energy minimization and checked for correctness using Ramachandran plot and ERRAT, which showed a good quality model of 91.6 and 65.0%, respectively. The protein model was used to preform MD simulation and docking of palmitic acid using CHARMM36 force field in GROMACS Version 5 and Autodock tool Version 4.2, respectively. The docking simulation with the lowest binding energy, -6.8 kcal/mol had a number of residues in close contact with the docked palmitic acid namely, Ile26, Tyr95, Val179, Gly180, Pro64, Glu203, His34, His206, His71, Arg182, Thr85, Lys98 and His177. Interestingly, among the binding residues are His34, His71 and His206 from the first, second, and third conserved histidine motif, respectively

which constitute the active site of the enzyme. The results obtained are in compliance with the in vivo activity of the Δ9-fatty acid desaturase on the membrane phospholipids.

# Homology Modeling and Docking studies of a Δ9-fatty acid desaturase from a Cold-tolerant *Pseudomonas* sp. AMS8

Lawal Garba[1, 2,3], Mohamad Ariff Mohamad Yussoff[4], Khairul Bariyyah Abd Halim[4], Siti Nor Hasmah Ishak[1], Mohd Shukuri Mohamad Ali[1,5], Siti Nurbaya Oslan[1,5] and Raja Noor Zaliha Raja Abdul Rahman*[1,2]

1. Enzyme and Microbial Technology Research Centre, Faculty of Biotechnology and Biomolecular Sciences, Universiti Putra Malaysia, Serdang, Selangor, Malaysia.
2. Department of Microbiology, Faculty of Biotechnology and Biomolecular Sciences, Universiti Putra Malaysia, Serdang, Selangor, Malaysia.
3. Department of Microbiology, Faculty of Science, Gombe State University, Gombe, Gombe State, Nigeria.
4. Department of Biotechnology, Kulliyyah of Science, International Islamic University Malaysia, Kuantan, Pahang Darul Makmur, Malaysia.
5. Department of Biochemistry, Faculty of Biotechnology and Biomolecular Sciences, Universiti Putra Malaysia, Serdang, Selangor, Malaysia.

*Correspondence author:

Raja Noor Zaliha Raja Abd. Rahman,

Enzyme and Microbial Technology Research Centre, Faculty of Biotechnology and Biomolecular Sciences, Universiti Putra Malaysia, 43400 UPM Serdang, Selangor Darul Ehsan, Malaysia

Phone number: +60192760708

Email: rnzaliha@upm.edu.my

**Abstract**

Membrane-bound fatty acid desaturases perform oxygenated desaturation reactions to insert double bonds within fatty acyl chains in regioselective and stereoselective manners. The Δ9-fatty acid desaturase strictly creates the first double bond between C9 and 10 positions of most saturated substrates. As the three-dimensional structures of the bacterial membrane fatty acid desaturases are not available, relevant information about the enzymes are derived from their amino acid sequences, site-directed mutagenesis and domain swapping in similar membrane-bound desaturases. The Cold-tolerant *Pseudomonas* sp. AMS8 was found to produce high amount of monounsaturated fatty acids at low temperature. Subsequently, an active Δ9-fatty acid desaturase was isolated and functionally expressed in *Escherichia coli*. In this paper we report the homology modeling and docking studies of a Δ9-fatty acid desaturase from a Cold-tolerant *Pseudomonas* sp. AMS8 for the first time to the best of our knowledge. Three dimensional structure of the enzyme was built using MODELLER version 9.18 using a suitable template. The protein model contained the three conserved-histidine residues typical for all membrane-bound desaturase catalytic activity. The structure was subjected to energy minimization and checked for correctness using Ramachandran plot and ERRAT, which showed a good quality model of 91.6 and 65.0%, respectively. The protein model was used to preform MD simulation and docking of palmitic acid using CHARMM36 force field in GROMACS Version 5 and Autodock tool Version 4.2, respectively. The docking simulation with the lowest binding energy, -6.8 kcal/mol had a number of residues in close contact with the docked palmitic acid namely, Ile26, Tyr95, Val179, Gly180, Pro64, Glu203, His34, His206, His71, Arg182, Thr85, Lys98 and His177. Interestingly, among the binding residues are His34, His71 and His206 from the first, second, and third conserved histidine motif, respectively which constitute the active site of the enzyme. The results obtained are in

compliance with the *in vivo* activity of the Δ9-fatty acid desaturase on the membrane phospholipids.

## Introduction

Fatty acid desaturase enzymes perform desaturation reactions which strictly create a double bond within fatty acyl chain in regioselective and stereoselective manners. Phylogenetically, the enzymes have been broadly divided into two unrelated classes as the acyl-acyl carrier protein and membrane-bound fatty acid desaturases. The class of the acyl-acyl carrier proteins specifically catalyses the production of oleic acid (C18:1) from stearic acid (C18:0) in plants whereas that of the membrane-bound desaturases represent the most widely distributed form of the enzymes predominantly found in bacteria and eukaryotes (Hashimoto *et al.*, 2008; Kachroo *et al.*, 2007).

In the mechanism of oxygen-dependent desaturation reactions, the fatty acid desaturases activate molecular oxygen using their active-site diiron centre which is shared by several proteins such as ribonucleotide reductase, methane monooxygenase, rubrerythrins, and a range of oxidase enzymes. Relevant information about the tuning of the diiron centers in relation to various chemical reactivity have been made available through comparisons of the diiron clusters of many diiron-containing enzymes (Sazinsky and Lippard, 2006; Shanklin *et al.*, 2009; Yoon and Lippard, 2004). Nevertheless, disparities in various protein to protein interactions, amino acid sequence and reaction outcomes confound the analysis. Research on fatty acid desaturases and similar enzymes created an avenue to conducting structure-function analyses due to a wide range of reactions performed on like substrates by the close homologous enzymes (Lee *et al.*, 1998; Shanklin and Cahoon, 1998; Shanklin *et al.*, 2009).

The amino acid sequences of both the integral membrane desaturases in (bacteria and eukaryotes) and acyl-acyl carrier protein desaturases of plants contain conserved histidine boxes predicted as the essential catalytic sites of the enzymes (Alonso *et al.*, 2003). However, the former enzymes contained three conserved-histidine motifs labelled as 'HXXXXH', 'HXXHH' and HXXHH' whereas the latter contained twice conserved-histidine motifs as EXXH (Alonso *et al.*, 2003; Lindqvist *et al.*, 1996) . As the three-dimensional structures of the bacterial membrane fatty acid desaturases are still unavailable, relevant information about the enzymes are derived from the amino acid sequences, site-directed mutagenesis, and domain swapping in similar membrane-bound desaturases coupled with homology modelling(Venegas-Calerón *et al.*, 2006). The Cold-tolerant *Pseudomonas* sp. AMS8 was able to produce high amount of monounsaturated fatty acids at 4 $^{o}$C (Lawal *et al.*, 2016). Subsequently, an active Δ9-fatty acid desaturase was isolated and functionally expressed in *Escherichia coli.* The enzyme was found to catalyse conversion from membrane associated palmitic to palmitoleic acid (Garba *et al.*, 2016a). In this paper we report homology modeling and docking studies of Δ9-fatty acid desaturase from a Cold-tolerant *Pseudomonas* sp. AMS8 with palmitic acid as a substrate for the first time to the best of our knowledge.

## Materials and Methods

### Templates selection

BLASTP of the target protein was performed at the NCBI (https://blast.ncbi.nlm.nih.gov/Blast.cgi?PROGRAM=blastp) which showed 24 and 23% similarities to human integral membrane stearoyl-CoA desaturase (PDB ID: 4ZYO) and mouse stearoyl-coA desaturase (PDB ID: 4YMK), respectively. However, the mouse stearoyl-coA desaturase

(PDB ID: 4YMK) was chosen as a template (based on its high resolution) to predict the three dimensional structure of the Δ9-fatty acid desaturase.

**Structure prediction**

The primary sequences of human (Uniprot ID:O00767) and mouse (Uniprot ID:P13516) desaturases were obtained from Uniprot protein databases. Moreover, the protein sequences of Δ9-fatty acid desaturases from several other *Pseudomonas* species were obtained from the GenBank. The transmembrane (TM) spanning region of *Pseudomonas* sp. AMS8 Δ9-fatty acid desaturase was predicted using a TM domain topology prediction program, CCTOP (http://cctop.enzim.ttk.mta.hu/). The CCTOP predicted the TM domains of the protein sequence based on the consensus of ten (10) different methods (Dobson *et al.*, 2015a, 2015b). The TM domains were modelled together with the remaining amino acid residues toward the C-terminus of the protein using MODELLER version 9.18 (Webb and Sali, 2014). Alignment input used in the MODELLER was derived from the pairwise alignments of both the template and model primary sequences using membrane proteins alignment tool (Stamm *et al.*, 2013) whereas the secondary structure was predicted using PSIPRED tool (Buchan *et al.*, 2013) and used as a guide to modelling the C-terminal domain.

**Energy minimization and Quality verification**

The protein model generated by the MODELLER was ranked and scored using discrete optimised protein energy (DOPE) score. The top three models out of 50 models with the lowest DOPE scores were chosen and assessed using ERRAT and RAMPAGE server. The best model was selected for energy minimization to remove clashes between side chains using GROMACS and subsequently used in docking and molecular dynamics simulations. Further structural assessment was performed by simulating the homology models inside a membrane bilayer.

**Active site Prediction**

Prior to docking simulations, the binding site for the *Pseudomonas* sp. AMS8 model was predicted using COACH (Buchan *et al.*, 2013). The predicted active site was found in the vicinity of histidine rich region, which served as an already established potential binding site of the enzyme (this site was used for a targeted docking). Blind docking was also performed to bind palmitate on both the template and model structures.

**Docking studies**

Three dimensional (3D) structure of palmitic acid was obtained from the Pubchem (https://pubchem.ncbi.nlm.nih.gov). The energy minimized model of the Δ9-fatty acid desaturase and the palmitic acid (ligand) were prepared and used for molecular docking of the substrate onto the target proteins using Autodock tool Version 4.2 (Trott and Olson, 2010). Blind docking of the palmitate onto the modelled structure was performed using a pre-set simulation grid box size of 126x126x126 Å along the X,Y and Z axes and centred at 39.946,40.191,45.879 whereas the targeted docking grid box size was set to 70x70x60 Å dimension and centred at 43.946, 40.191,33.879 of X,Y and Z coordinate, respectively. The docking simulations were performed for 100 runs using Lamarckian Genetic Algorithm (LGA). The results were evaluated using RMSD values, ligand-protein interactions, binding energy ($\Delta G_{bind}$) as well as a number of conformations existed in a populated cluster. The charge values of metal ions have been indicated to play a crucial role in predicting correct docking simulations. Previous report showed that different charge values of magnesium ions were verified and found a charge of +2 as too high, causing it to diminish due to partial binding of the adjacent groups (Chen *et al.*, 2017). A docking study conducted on

149 dioxyhypusine hydroylase (DOHH) with its substrate in the presence of Fe-Fe confirmed that
150 Fe charge of +1 produced substrate binding mode which sufficiently agreed with the
151 experimental data. Thus, in this study, iron charges of 0 (default charge in Autodock), +1 and
152 +2 were tested in the docking simulations for comparison. The ligand-protein interaction was
153 visualized using Pymol (Trott and Olson, 2010) and VMD (Humphrey *et al.*, 1996).

154 **MD simulations**

155 The model structure of the Δ9-fatty acid desaturase was simulated in an embedded 1-
156 palmitoyl-2-oleoyl-sn-glycero-3-phosphocholine (POPC) bilayer. The protein-bilayer system
157 was constructed using CHARMM-GUI Membrane builder (Jo *et al.*, 2008). The atomistic
158 MD simulations were performed using CHARMM36 force field (Huang and MacKerell,
159 2013) in GROMACS Version 5 (Pronk *et al.*, 2013) within an integration time step of 20 fs.
160 The simulation temperature was kept constant at 310 K by coupling the system to a heat bath
161 using a Nose-Hoover thermostat with $\tau_T$ = 1 ps. Pressure was maintained at 1 atm using a
162 Parinello-Rahman barostat and semiisotropic pressure with $\tau_P$ = 5 ps and a compressibility of
163 $4.5e^{-5}$ bar $^{-1}$. Long-range electrostatics was treated using particle mesh Ewald method with a
164 cutoff of 12 Å. The 12 Å cutoff distance was used for van der Waals interactions. The
165 systems were equilibrated for 1 ns restraining the Cα atoms, followed by production runs of
166 50 ns each in triplicates. The data was analysed using GROMACS tools and VMD.

167 **Results**

168

169 **Sequence of the Δ9-fatty acid desaturase protein and templates identification**
170

171 The Δ9-fatty acid desaturase was isolated from a Cold-tolerant *Pseudomonas* sp. AMS8 and
172 functionally expressed in *Escherichia coli* as confirmed by GCMS analysis which showed an
173 active enzyme capable of increasing the overall palmitoleic acid content of the recombinant

*E. coli*. Based on the GCMS analysis, a profound increase of the amount of palmitoleic acid from 10.5 to 21% was observed at 20 $^{o}$C (Garba *et al.*, 2016a). The protein had a molecular weight of 45 kDa and 394 amino acids which was already deposited at NCBI (accession number: AMX81567). Multiple sequences alignments of the template, the Cold-tolerant *Pseudomonas* sp. AMS8 Δ9-fatty acid desaturase and sequences from several other Δ9-fatty acid desaturases has revealed the three conserved-histidine boxes common to all membrane-bound desaturases in bacteria (Garba *et al.*, 2016b; Li *et al.*, 2009), fungi (Chen *et al.*, 2013) and animals (Bai *et al.*, 2015) (Figure 1). The human integral membrane stearoyl-CoA desaturase (PDB ID: 4ZYO) and mouse stearoyl-coA desaturase (PDB ID: 4YMK) have been solved to a resolution of 3.25 Å and 2.6 Å, respectively. The two structures share moderate sequence identities of 24 and 23% with the *Pseudomonas* sp. AMS8, respectively. However, the mouse stearoyl-coA desaturase was chosen as the template based on its higher resolution.

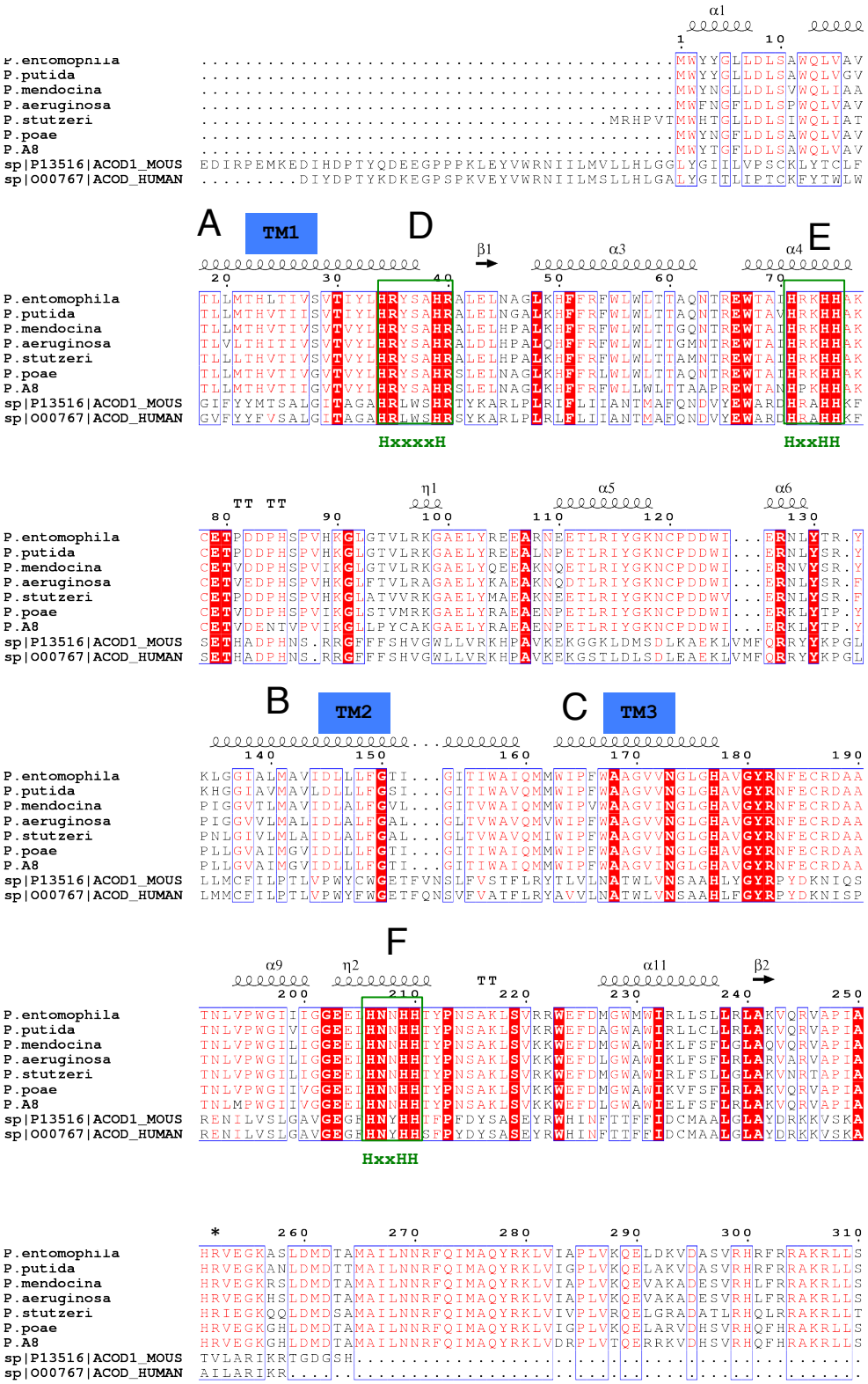
α1
P.entomophila
P.putida
P.mendocina
P.aeruginosa
P.stutzeri
P.poae
P.A8
sp|P13516|ACOD1_MOUS
sp|O00767|ACOD_HUMAN
A
TM1
D
β1
α3
E
α4
HxxxxH
HxxHH
η1
α5
α6
TT TT
B
TM2
C
TM3
F
α9
η2
TT
α11
β2
HxxHH

Figure 1: Multiple sequences alignments of protein sequence from *Pseudomonas* sp. AMS8 Δ9-fatty acid (AMX81567) and sequences from other desaturase proteins. The transmembrane domains of the protein are indicated by letters A, B and C whereas the three conserved-histidine boxes common to all membrane-bound desaturases are shown by D, E, and F. The end of the model structure is at Arg252 indicated by an asterisk (*).

**Model of the Δ9-fatty acid desaturase**

To correctly model the TM domain of a membrane protein, it is necessary to appropriately predict its TM spanning region. CCTOP used 11 TM prediction programs including some of the best TM domain predictor such as TMHMM and HMMTOP to predict the TM domain of the target protein. Most of the prediction programs predicted that the target protein has three TM spanning regions as detailed in Figure 2A, which gave a consensus domains of TM1 (Leu13——Leu33), TM2 (Leu135——Ile159) and TM3 (Met162——Tyr181) of 20, 25 and 20 amino acid residues, respectively. However, the TM2 and TM3 were not aligned at the TM domains of the template. Thus, some manual adjustment of the TM2 and TM3 was performed to prepare the alignment input for the MODELLER. As the three dimensional (3D) structure of the template had four TM domains, only three TM3 domains were considered for modelling the P*seudomonas* sp. AMS8 Δ9-fatty acid desaturase (predicted to have only three TM domains) using MODELLER (Figure 2B). The structure with the lowest DOPE score was assessed and improved after energy minimization and subsequently used for further analyses.

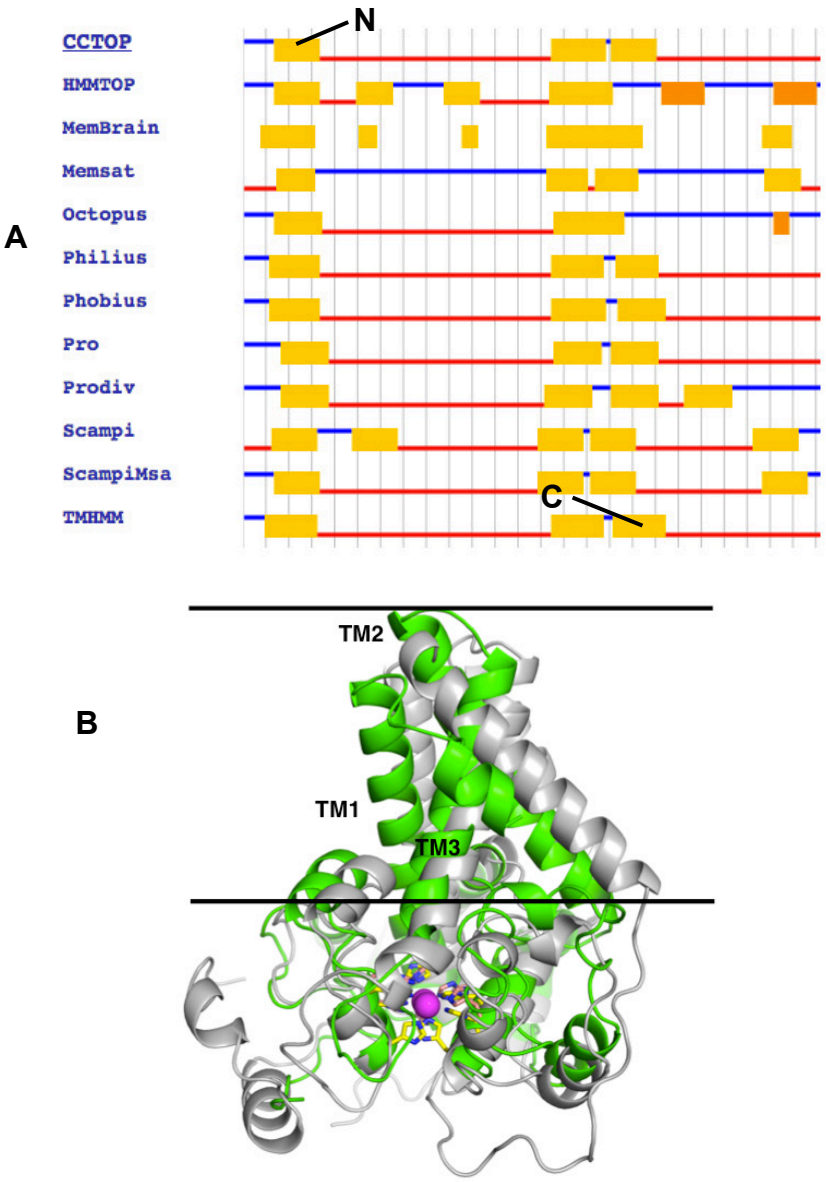


Figure 2: The TM topology as derived from CCTOP prediction A). Superimposed three dimensional model structures of *Pseudomonas* sp. AMS8 Δ9-fatty acid desaturase (green) and the template from the crystal structure of mouse stearoyl-coenzyme A desaturase (4YMK) shown in grey (B). The Zn ions found in the crystal structure of the mouse desaturase are shown as purple spheres. The approximate position of the bilayer is indicated by the two black lines.

**Quality verification of the predicted structure**

Quality of protein models are verified using various programmes such as ERRAT and Ramachandran plot which are freely available online servers (Colovos and Yeates, 1993). In this study, the predicted structure that has gone through energy minimization was verified for correctness using the ERRAT and Ramachandran plot and labelled as AMX8-em (shown in the supplementary files). The ERRAT programme showed an overall quality value of 65.021% for this structure (Figure 3). In general, at lower resolution, more than 92% of the surveyed structures had more than 80% of their residues outside the 95% exclusion zone (Colovos and Yeates, 1993). RAMPAGE programme is used to check the overall sterio-chemical quality, local and residue-by-residue reliability usually shown on a Ramachandran plot. The programme shows the sterio-chemistry of the main-chain torsion angles Phi, Psi (φ, ψ) of a good protein model. The Ramachandran plot displays the polypeptide chain of a protein structure using the φ, ψ angles pair (Laskowski *et al.*, 1993; Mahgoub and Bolad, 2013; Ramachandran *et al.*, 1963). Figure 4 and Table 1 indicate that up to 91.6% of the residues fall within the most favoured regions, 6.8% in the allowed regions whereas only 1.6% residues are in the outlier regions, further confirming that the predicted model is of good quality.

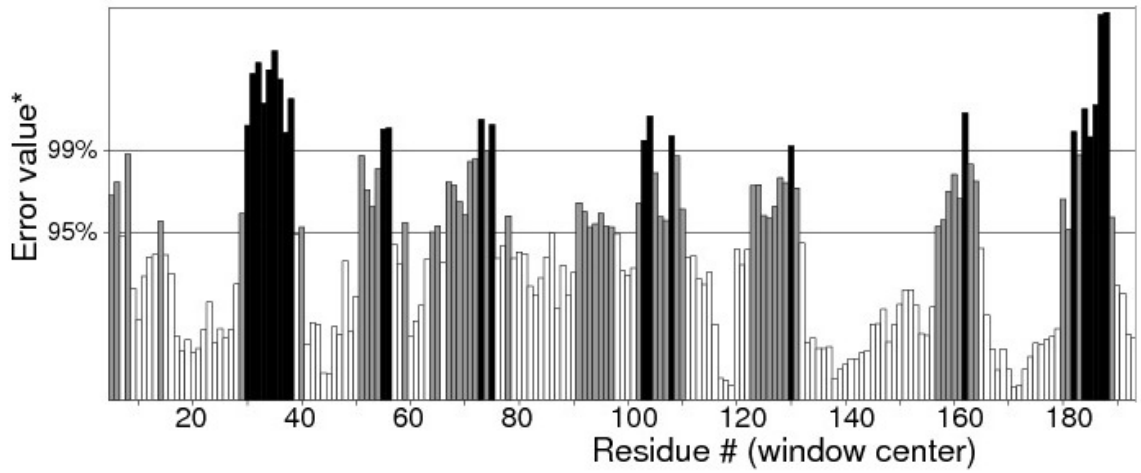


Figure 3: Quality verification plot of the energy minimized model of the Δ9-fatty acid desaturase performed using ERRAT. The two lines drawn on the error axis show the confidence with which it is possible to reject regions that exceed that error value. In good high resolution structures, 95% or more of the amino acids lie below the 95% threshold whereas in lower resolution (2.5-3Å) structures around 91% of the amino acids lie below that threshold.

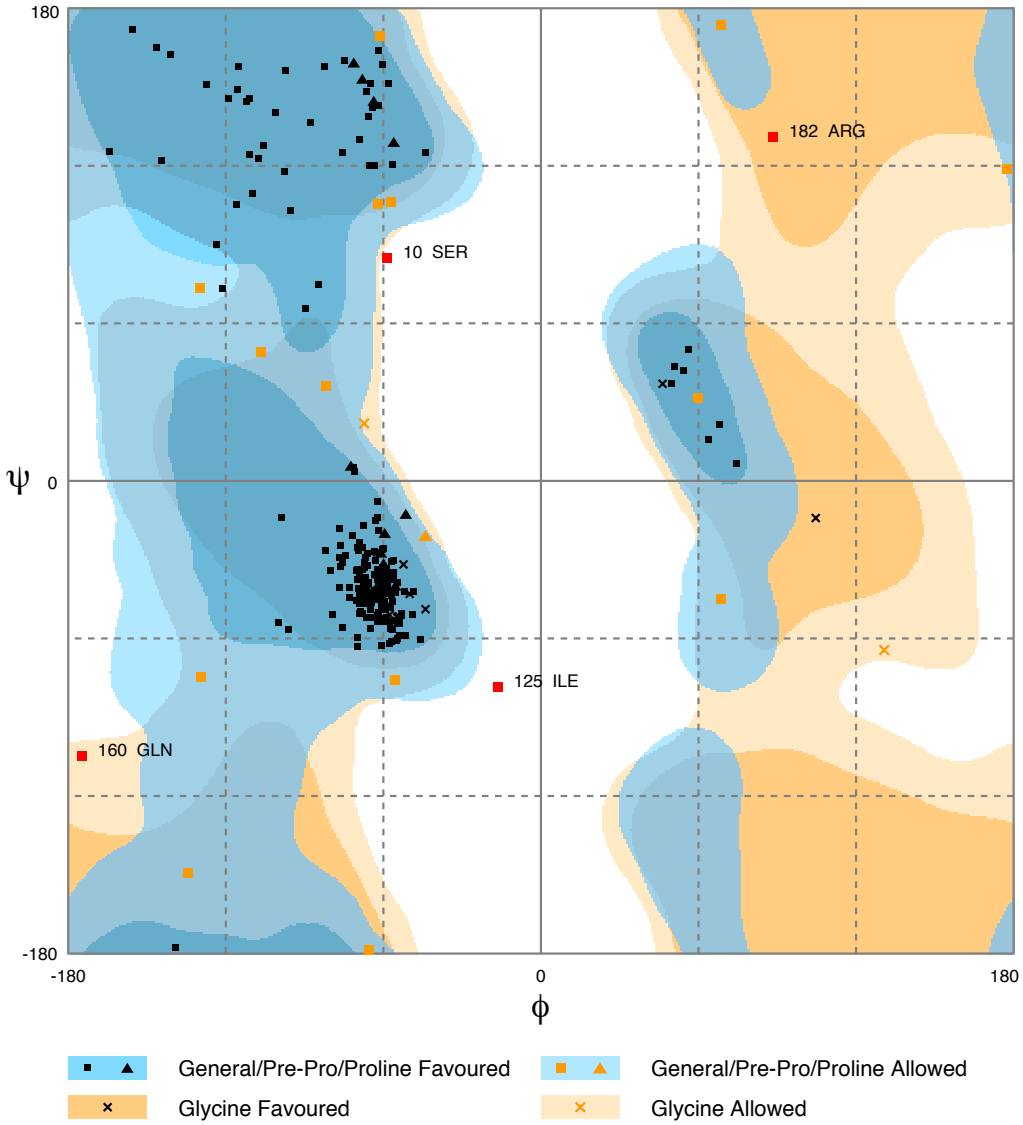


Figure 4: Ramachandran plot of *Pseudomonas* sp. AMS8 Δ9-fatty acid desaturase model generated by RAMPAGE server.

Table 1: Details of Ramachandran plot after energy minimization

| Plot statistics | % after energy minimization |
|---|---|
| Residues in the most favoured regions | 91.6 |
| Residues in allowed regions | 6.8 |
| Residues in the outlier region | 1.6 |

**Catalytic site of the predicted structure**

Membrane-bound desaturases share an exceptional structural resemblance and a wide range of functionality. Three conserved-histidine boxes that are common to all classes of these

298 enzymes function in binding two irons at the catalytic centre. The structural similarity has
299 given an insight into their structure-function relationships (Meesapyodsuk *et al.*, 2007). The
300 predicted structure of *Pseudomonas* sp. AMS8 Δ9-fatty acid desaturase contains the three
301 conserved-histidine boxes consisting of eight histidine residues at positions 1 (His34, His39),
302 2 (His71, His74, His75) and 3(His206, His209, His210) from N to C-terminus of the enzyme
303 shown in Figure 5A and analysed in Figure 5B. The conserved-histidine motifs are consistent
304 with those observed during the multiple sequences alignments of the target sequence with the
305 template corresponding to the already established catalytic centre of membrane-bound
306 desaturases. The role of the eight histidine residues in the conserved histidine-rich motifs has
307 been demonstrated through site-directed mutagenesis of rat stearoyl-CoA $\Delta^9$-desaturase
308 whereas those residues flanking the conserved region have critical catalytic properties in
309 plant FAD2 desaturases and related enzymes (Broadwater *et al.*, 2002; Meesapyodsuk *et al.*,
310 2007; Shanklin *et al.*, 1994).

311

312

313

314

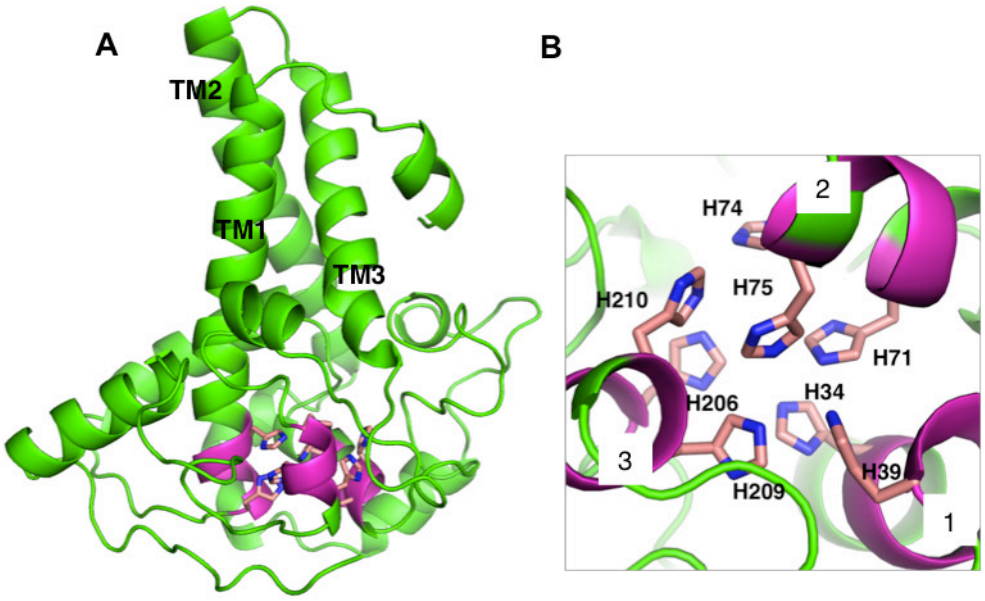


Figure 5: Analysis of *Pseudomonas* sp. AMS8 Δ9-fatty acid desaturase model showing the overall cartoon representation of the structure, the transmembrane domains are labelled TM1, TM2 and TM3. The conserved histidine motifs are shown in magenta (A) and the bottom view of the putative catalytic-site residues with the Histidine residues shown in stick representation and the conserved histidine motifs are labelled as 1,2, and 3 (B).

**Docking studies**

The membrane-bound Δ9-fatty acid desaturase uses activated oxygen molecule to create double bond between C-H bonds of saturated substrates. The enzyme particularly introduces double bond at Δ9-position of saturated palmitic and stearic acids to produce palmitoleic and oleic acids, respectively serving as the fundamental substrates for phospholipids construction and other complex lipid molecules (Castro *et al.*, 2011).

To investigate substrate specificity of *Pseudomonas* sp. AMS8 Δ9-fatty acid desaturase, docking studies of palmitic acid onto the modeled structure and the template were performed using Autodock software. Blind docking of palmitate and the template was first performed which showed that the palmitate was docked on the template at a site different from the vicinity of the template catalytic site observed for its native ligand. Similarly, for the model

334 structure of desaturase from *Pseudomonas* AMS8, the docked conformation with lowest
335 docking energy formed close contact with Thr4, Trp167, Val171, Gly170, Leu175, Ala63,
336 Cys96, Gly174, Tyr95, Met141, Ile144, and Ile140 outside the catalytic site. This is expected
337 as the COACH predicted multiple binding sites on the protein.

338 It is known that the potential catalytic and binding sites for palmitate are close to the His
339 conserved motif. Therefore, specific docking was performed with grid box which covers the
340 histidine residues of the motifs. The docking simulation which produced the lowest binding
341 energy, -6.8 kcal/mol is depicted in Figure 6A. A number of residues were found in close
342 contact with the docked palmitic acid namely, Ile26, Tyr95, Val179, Gly180, Pro64, Glu203,
343 His34, His206, His71, Arg182, Thr85, Lys98 and His177 (Figure 6B). Interestingly, among
344 the binding residues are His34 and His71 and His206 from the first, second, and third
345 conserved histidine motif of the enzyme, respectively. The ligand formed two hydrogen
346 bonds with Lys98 and His177. These suggest that the docked substrate was very close to the
347 enzyme catalytic site and the conserved-histidine residues holding the metal ions of
348 membrane-bound desaturases which are known to play a key role for the enzymes catalytic
349 activity (Shanklin *et al.*, 2009).

350

351

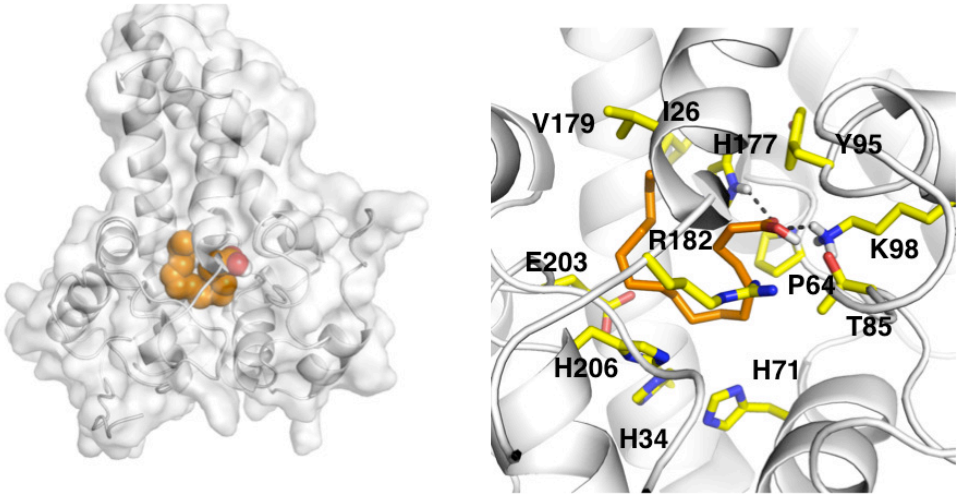


Figure 6: Docking studies of the 3D structure of palmitic acid onto the predicted model of the Δ9-fatty acid desaturase. The protein-ligand interactions are shown in surface (A) and the residues involved in binding the ligand (B) analysed using PyMOL software. Two potential hydrogen bonds predicted between Lys98 (K98) and His177 (H177) and palmitate are shown as dotted black lines.

To ascertain the role of the metal irons on the membrane-bound fatty acid desaturases, docking simulations were performed on both the model (Figure 7) and template (Figure 8) structures in the presence and absence of metal irons at their catalytic sites. Using the Autodock, different docking scores were predicted and summarized in (Table 2).Lowest docking energy (-6.81) was observed when the palmitate was docked onto the model in the presence of metal irons, which suggests a more favourable configuration (Figure 9). However, the control docking simulations performed on the template with the palmitate in the presence and absence of the iron metals showed much higher docking energies of -6.21 and 5.82, respectively, which indicate that the palmitate was unfavourably bound to the mouse desaturase enzyme catalytic site even in the presence of the metal irons.

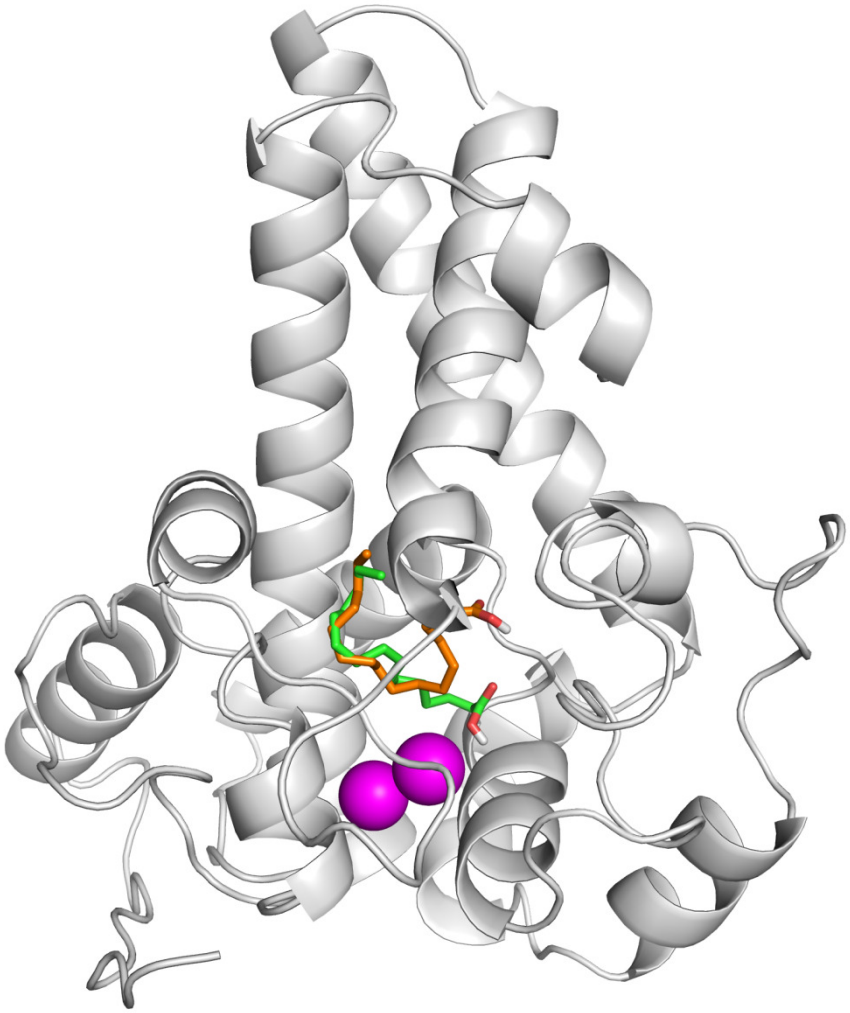

Figure 7: Superpose of ligand binding mode on the target site of the model structure. The palmitate is shown using stick representation in the presence of di-iron (C atom in green) and in the absence of the di-iron (C atom in orange) with O and H atoms in red and white, respectively. The di-irons are shown in purple spheres. Positions of the irons were estimated based on their locations in the template structure (PDB ID:4ymk).

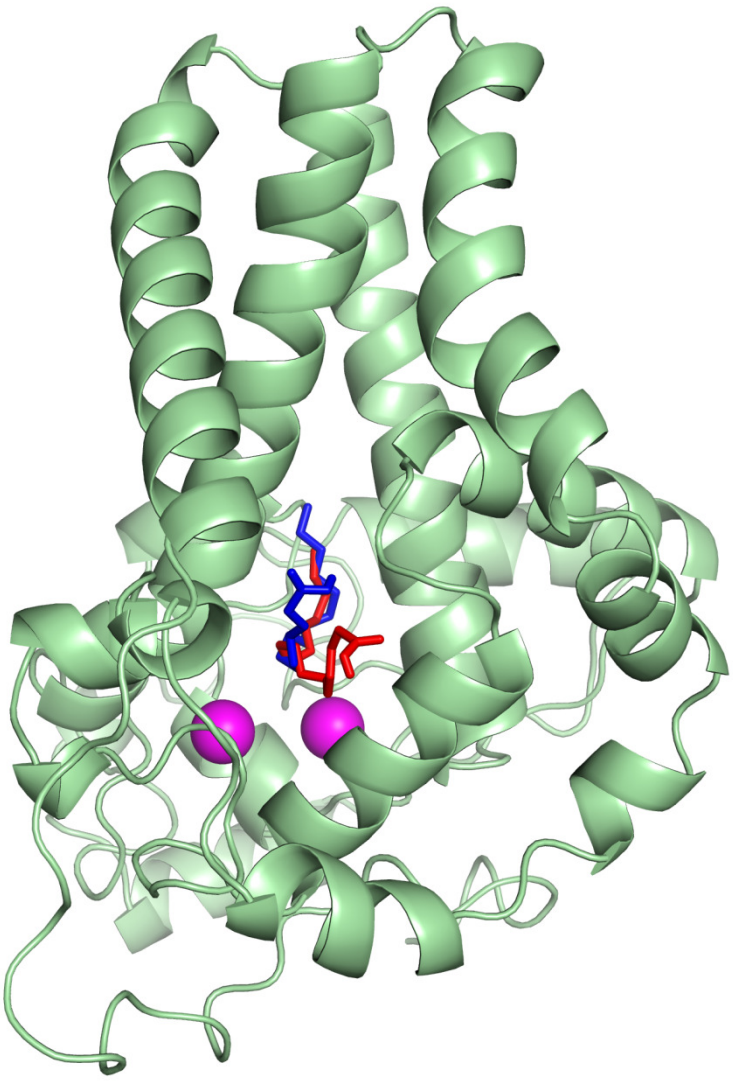

Figure 8: Superpose of the palmitate binding mode on the active site of the template (PDB ID:4ymk) in the presence (red) and absence of di-iron (blue). The ligands are shown in stick representation and the di-iron as purple spheres.

Table 2: Summary of docking simulations performed using Autodock

| System | Autodock score (*) | Amino acid residues involved in hydrogen bond interactions |
|---|---|---|
| Model + Palmitate + di-iron (default charge, 0) | -6.81 | Arg65, His71 |
| Model + Palmitate + di-iron (charge = +1) | -6.48 | Arg65, His71 |
| Model + Palmitate + di-iron (charge = +2) | -6.74 | Arg65, His71 |
| Model + Palmitate | -6.26 | Arg65, His71 |
| 4YMK + Palmitate+di-iron | -6.27 | Asn144 |
| 4YMK + Palmitate | -5.82 | Trp258 |

*the scores were selected based on the highest conformation observed in the docking simulations.

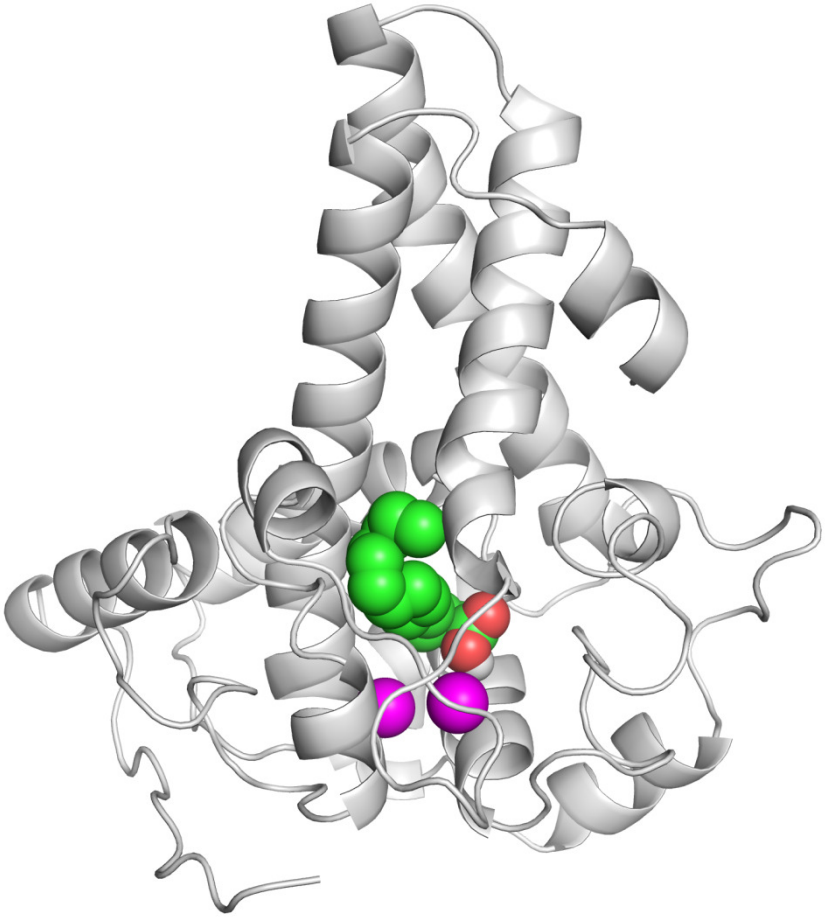

Figure 9: The docked palmitate on the active site of the model structure in the presence of di-iron. The ligand is shown as spheres with C, O and H atoms in green, red and white, respectively. The di-iron is shown as purple spheres.

**Simulation of the predicted model of the Δ9-fatty acid desaturase in membrane**

In order to further assess the Δ9-fatty acid desaturase model, the protein was embedded within a POPC bilayer and simulated for 50 ns. The approximate location of the bilayer was predicted based on the position of bilayer of the template structure. During equilibration, the protein movement was restrained for 1 ns to allow lipid molecules to equilibrate around the protein. The initial structure of the protein inside the POPC bilayer and its final structure at the end of the MD simulation are shown in Figure 10.

399

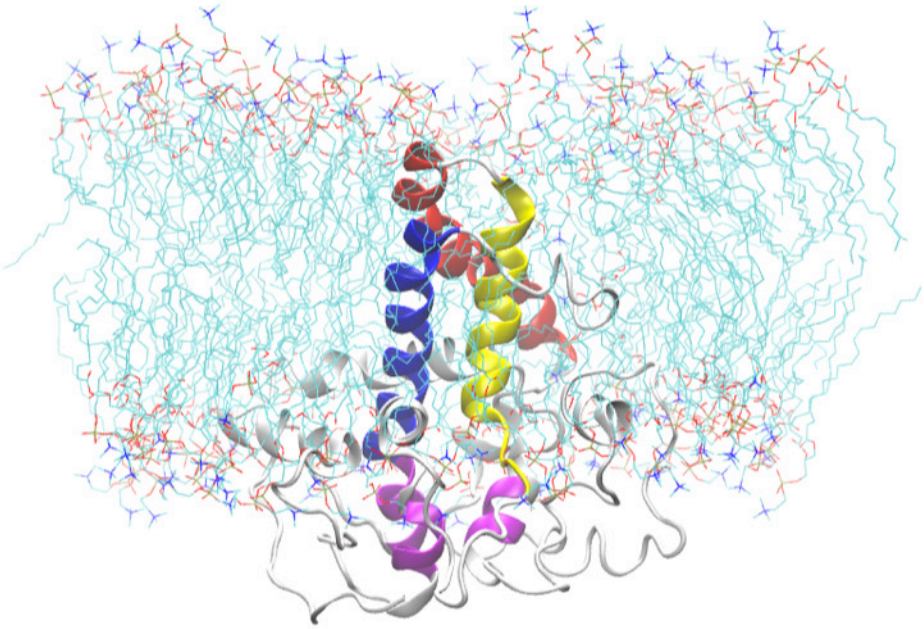

400

401 Figure 10: A snapshot of the atomistic MD simulation of the Δ9-fatty acid desaturase in
402 POPC lipid bilayer at t=50 ns. The protein is shown in cartoon representation in grey with the
403 TM domains coloured as blue, red, and yellow for TM1, TM2 and TM3, respectively. The
404 conserved histidine motifs are highlighted in magenta. The POPC lipid molecules are shown
405 in line representation with carbon, nitrogen and oxygen atoms in cyan, blue and red
406 respectively. Water molecules are hidden for clarity.

407 In the membrane, the protein root mean square deviation (RMSD) was calculated to check
408 the overall structure stability (Figure 11). The RMSD underwent major changes in the first 5
409 ns and became more stable after 20 ns. To ascertain the real cause of the significant changes
410 observed during the MD simulation, a more fine-grained analysis of the RMSD of the entire
411 protein and its different regions [specifically the TM domains 1 to 3, and the C-terminal
412 region following the last residue of TM3 (182 to 252) of the model structure] along the
413 simulation was carried out. The RMSD established an overall stable protein, which is well
414 equilibrated in the POPC bilayer after the 20 ns. The pdb coordinates of the protein analysed
415 at 25, 30 and 50 ns were extracted from the MD trajectory and performed ERRAT analyses
416 which showed overall quality scores of 90.81, 93.33 and 84.74%, respectively (Figure 12).

417

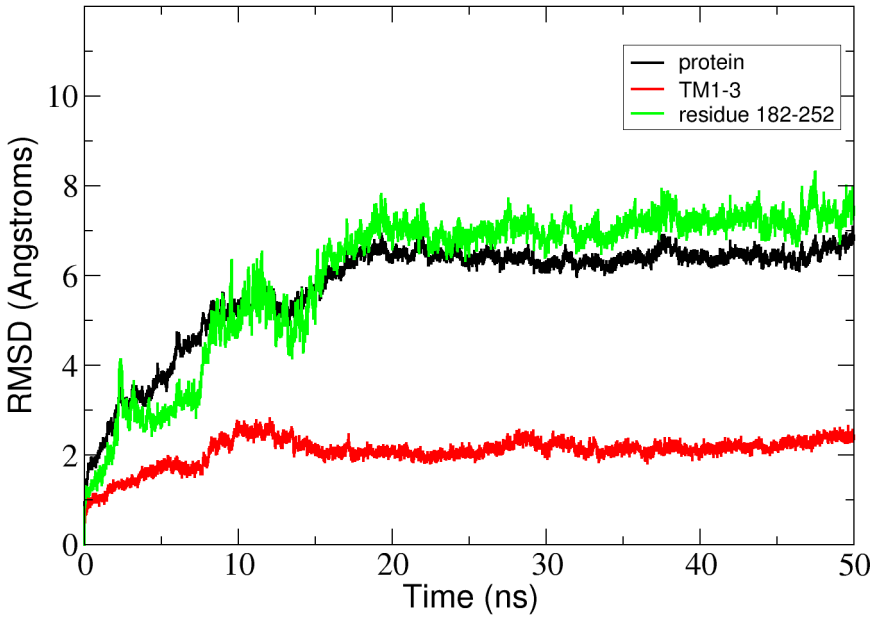


Figure 11: Total RMSD of the Δ9-fatty acid desaturase simulated in POPC lipid bilayer and RMSD of its different regions simulated in a POPC lipid bilayer.

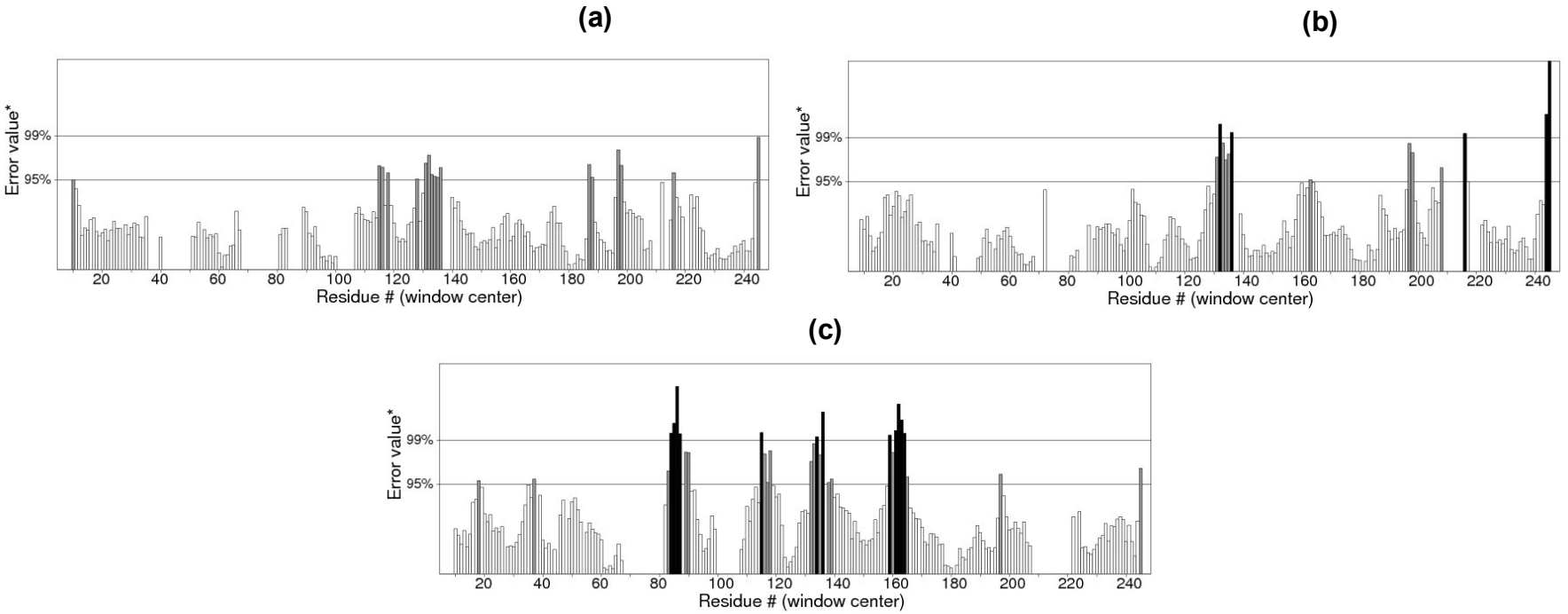


Figure 12: ERRAT analyses of the structures at 25 ns (a), 30 ns (b) and 50 ns (c) which produced overall quality scores of 90.81, 93.33 and 84.74%, respectively.

**Discussion**

Fatty acid desaturase enzymes are involved in unsaturated fatty acid synthesis through desaturation reactions and usually have specificity for double bond insertion along the saturated acyl chains (Los and Murata, 1998; Wang *et al.*, 2013). Membrane-bound fatty acid desaturases perform dehydrogenation reactions of fatty acyl chains that are non-heme di-iron and oxygen-dependent (Meesapyodsuk *et al.*, 2007). Contrary to soluble fatty acid desaturases which have been extensively studied, structural information about the membrane-bound fatty acid desaturases is very limited. Membrane-bound fatty acid desaturases have been isolated and characterised from bacteria (Garba *et al.*, 2016a; Li *et al.*, 2008), fungi (Chen *et al.*, 2013), plants (Gao *et al.*, 2014; García-Maroto *et al.*, 2002) and animals (Bai *et al*., 2015; Wang *et al*., 2015). However, the only membrane-bound fatty acid desaturases that have been crystallised so far were reported from animals such as mouse stearoyl-CoA desaturase (Bai *et al*., 2015) and human stearoyl-CoA desaturase (Wang *et al*., 2015). Both the primary sequence and the modelled structure of the *Pseudomonas* sp. AMS8 Δ9-fatty acid desaturase revealed the presence of three conserved-histidne residues at positions 34-39, 71-75 and 206-210, which are typical for all membrane-bound desaturases and play a vital role for the enzymes catalytic activity (Shanklin *et al.*, 2009) as shown in Figure 1 and Figure 5, respectively. Moreover, multiple sequences alignments of the template and the target showed an extension of amino acids (Val 253 to Ala394) at the C-terminal tail of the target which is completely not observed in the template. Therefore, only residues 1 to 252 were included in the model structure. However, BlastP at NCBI showed that, the extension shares 93% identity to both aminotransferases and acyl-CoA desaturases of many *Pseudomonas* species.

Contrary to the crystallised structures of other membrane-bound desaturases such as the mouse stearoyl-CoA desaturase (Bai *et al*., 2015) and the human integral membrane stearoyl-CoA desaturase (Wang *et al*., 2015), which both had four (4) transmembrane domains, the modeled structure of the *Pseudomonas* sp. AMS8 Δ9-fatty acid desaturase has only three (3) transmembrane domains (Figure 2) which are thought sufficient enough to span the membrane bilayer twice with both protein termini facing the cytosol. Although to the best of our knowledge, there was no report on the biding residues for palmitic acid from membrane-bound Δ9-fatty acid desaturase, Ile26, Tyr95, Val179, Gly180, Pro64, Glu203, His34, His206, His71, Arg182, Thr85, Lys98 and His177 were found to bind this substrate (Figure 6). Among these residues, Ile, Val, Gly, and Arg are comparable to biding residues for stearoyl-CoA by the crystallised structure of a human stearoyl-Coenzyme A desaturase (Wang *et al*., 2015). Similarly, Arg, Ile, Val, Gly are comparable to some binding residues for stearoyl-CoA of a mammalian steayol-CoA desaturase (Bai *et al*., 2015).

**References**

Alonso DL, Garcia-Maroto F, Rodriguez-Ruiz J, Garrido J, Vilches M. 2003. Evolution of the membrane-bound fatty acid desaturases. *Biochemical systematics and ecology* 31(10):1111-1124.

Bai Y, McCoy JG, Levin EJ, Sobrado P, Rajashankar KR, Fox BG, Zhou M. 2015. X-ray structure of a mammalian stearoyl-CoA desaturase. *Nature*. 524(7564):252-256

Broadwater JA, Whittle E, Shanklin, J.2002. Desaturation and Hydroxylation residues 148 and 324 of arabidopsis fad2, in addition to substrate chain length, exert a major influence in partitioning of catalytic specificity. *Journal of Biological Chemistry* 277(18):15613-15620.

Buchan DW, Minneci F, Nugent TC, Bryson K, Jones DT. 2013. Scalable web services for the PSIPRED Protein Analysis Workbench. *Nucleic acids research 41*(W1), W349-W357.

Castro LFC, Wilson JM, Gonçalves O, Galante-Oliveira S, Rocha, E., Cunha, I. 2011. The evolutionary history of the stearoyl-CoA desaturase gene family in vertebrates. *BMC evolutionary biology* 11(1):1.

Chen D, Menche G, Power TD, Sower L, Peterson JW, Schein CH. 2007. Accounting for ligand-bound metal ions in docking small molecules on adenylyl cyclase toxins. *Proteins:Structure, Function, and Bioinformatics* 67:593-605.

Chen H, Gu Z, Zhang H, Wang M, Chen W, Lowther WT, Chen YQ. 2013. Expression and purification of integral membrane fatty acid desaturases. *PLoS ONE* 8(3): e58139.

Colovos C, Yeates, TO. 1993. Verification of protein structures: patterns of nonbonded atomic interactions. *Protein science* 2(9):1511-1519.

Dobson L, Reményi I, Tusnády GE. 2015a. CCTOP: a Consensus Constrained TOPology prediction web server. *Nucleic acids research, 43*(W1), W408-W412.

Dobson L, Reményi I, Tusnády, GE. 2015b. The human transmembrane proteome. *Biology direct* 10(1):31.

Gao L, Sun R, Liang Y, Zhang M, Zheng Y, Li D. 2014. Cloning and functional expression of a cDNA encoding stearoyl-ACP Δ9-desaturase from the endosperm of coconut (Cocos nucifera L.). *Gene,* 549(1):70-76.

Garba L, Ali MSM, Oslan SN, Rahman RNZRA. 2016a. Heterologous Expression of PA8FAD9 and Functional Characterization of a Δ9-Fatty Acid Desaturase from a Cold-Tolerant *Pseudomonas* sp. A8. *Molecular Biotechnology* 58(11):718-728.

Garba L, Ali MSM, Oslan SN, Rahman RNZRA.2016b. Molecular Cloning and Functional Expression of a Δ9-Fatty Acid Desaturase from an Antarctic *Pseudomonas* sp. A3. *PLoS ONE,* 11(8):e0160681.

García-Maroto F, Garrido-Cárdénas J, Rodríguez-Ruiz J, Vilches-Ferrón M, Adam A, Polaina J, López Alonso D. 2002. Cloning and molecular characterization of the Δ6-desaturase from two Echium plant species: Production of GLA by heterologous expression in yeast and tobacco. *Lipids* 37(4): 417-426. Doi: 10.1007/s1145-002-0910-6

Han Z, Sakai N, Böttger LH, Klinke S, Hauber J, Trautwein AX, Hilgenfeld R. 2015. Crystal Structure of the peroxo-diiron(III) Intermediate of deoxyhypusine hydroxylase, an oxygenase involved in hypusination. Structure 23(5):882-892

Hashimoto K, Yoshizawa AC, Okuda S, Kuma K, Goto S, Kanehisa M. 2008. The repertoire of desaturases and elongases reveals fatty acid variations in 56 eukaryotic genomes. *Journal of lipid research,* 49(1):183-191.

Huang J, MacKerell AD. 2013. CHARMM36 all□atom additive protein force field: Validation based on comparison to NMR data. *Journal of computational chemistry* 34(25):2135-2145.

Humphrey W, Dalke A, Schulten K.1996. VMD: visual molecular dynamics. *Journal of molecular graphics* 14(1):33-38.

Jo S, Kim T, Iyer VG, Im W. 2008. CHARMM□GUI: a web□based graphical user interface for CHARMM. *Journal of computational chemistry,* 29(11):1859-1865.

Kachroo A, Shanklin J, Whittle E, Lapchyk L, Hildebrand D, Kachroo P. 2007. The Arabidopsis stearoyl-acyl carrier protein-desaturase family and the contribution of leaf isoforms to oleic acid synthesis. *Plant molecular biology* 63(2):257-271.

Laskowski RA, Moss DS, Thornton JM. 1993. Main-chain bond lengths and bond angles in protein structures. *Journal of molecular biology* 23*1*(4):1049-1067.

Lawal G, Wahhida L, Mohd Shukuri M. 2016. Siti Nurbaya O and Raja Noor Zaliha RAR. Unsaturated Fatty Acids in Antarctic Bacteria. *Research Journal of Microbiology* 11:146-152.

Lee M, Lenman M, Banaś A, Bafor M., Singh S, Schweizer M, Nilsson R, Liljenberg C, Dahlqvist A, Gummeson PO. 1998. Identification of non-heme diiron proteins that catalyze triple bond and epoxy group formation. *Science,* 280(5365):915-918.

Li Y, Dietrich M, Schmid RD, He B, Ouyang, P, Urlacher VB.2008. Identification and functional expression of a Δ9-fatty acid desaturase from *Psychrobacter urativorans* in *Escherichia coli*. *Lipids,* 43(3):207-213.

Li, Y, Xu X, Dietrich M, Urlacher VB, Schmid RD, Ouyang P, He B. 2009. Identification and functional expression of a Δ9 fatty acid desaturase from the marine bacterium *Pseudoalteromonas* sp. MLY15. *Journal of Molecular Catalysis B: Enzymatic* 56(2):96-101.

Lindqvist Y, Huang W, Schneider G, Shanklin J. 1996. Crystal structure of delta9 stearoyl-acyl carrier protein desaturase from castor seed and its relationship to other di-iron proteins. *The EMBO journal* 15(16):4081.

Los DA, Murata N. 1998. Structure and expression of fatty acid desaturases. *Biochimica et Biophysica Acta (BBA)-Lipids and Lipid Metabolism,* 1394(1):3-15.

Mahgoub EO, Bolad A.2013. Correctness and accuracy of template-based modeled single chain fragment variable (scFv) protein anti-breast cancer cell line (MCF-7). *Open Journal of Genetics* 3(03):183.

Meesapyodsuk D, Reed DW, Covello PS, Qiu X. 2007. Primary structure, regioselectivity, and evolution of the membrane-bound fatty acid desaturases of *Claviceps purpurea*. *Journal of Biological Chemistry* 282(28):20191-20199.

Pronk S, Páll S, Schulz R, Larsson P, Bjelkmar P, Apostolov R, Shirts MR, Smith JC, Kasson PM, van der Spoel D. 2013. GROMACS 4.5: a high-throughput and highly parallel open source molecular simulation toolkit. *Bioinformatics,* 29(7):845-854.

Ramachandran GN, Ramakrishnan C, Sasisekharan, V.1963. Stereochemistry of polypeptide chain configurations. *Journal of molecular biology 7*(1): 95-99.

Sazinsky MH, Lippard SJ.2006. Correlating structure with function in bacterial multicomponent monooxygenases and related diiron proteins. *Accounts of chemical research 39*(8):558-566.

Shanklin J, Cahoon EB. 1998. Desaturation and related modifications of fatty acids. *Annual review of plant biology* 49(1):611-641.

Shanklin J, Guy JE, Mishra G, Lindqvist Y.2009. Desaturases: emerging models for understanding functional diversification of diiron-containing enzymes. *Journal of biological chemistry* 284(28):18559-18563.

Shanklin J, Whittle E, Fox BG. 1994. Eight histidine residues are catalytically essential in a membrane-associated iron enzyme, stearoyl-CoA desaturase, and are conserved in alkane hydroxylase and xylene monooxygenase. *Biochemistry, 33*(43), 12787-12794.

Stamm M, Staritzbichler R, Khafizov K, Forrest LR. 2013. Alignment of helical membrane protein sequences using AlignMe. *PLoS ONE 8*(3), e57731.

Trott O, Olson A J.2010. AutoDock Vina: improving the speed and accuracy of docking with a new scoring function, efficient optimization, and multithreading. *Journal of computational chemistry,* 31(2):455-461.

Venegas-Calerón M, Muro-Pastor A, Garcés R, Martínez-Force E.2006. Functional characterization of a plastidial omega-3 desaturase from sunflower (*Helianthus annuus*) in cyanobacteria. *Plant Physiology and Biochemistry,* 44(10):517-525.

Wang M, Chen H, Gu Z, Zhang H, Chen W, Chen YQ. 2013. ω3 fatty acid desaturases from microorganisms: structure, function, evolution, and biotechnological use. *Applied microbiology and biotechnology,* 97(24):10255-10262.

Webb B, Sali A. 2014. Protein structure modeling with MODELLER. *Protein Structure Prediction*, 1-15.

Yoon S, Lippard SJ. 2004. Water-dependent reactions of diiron (II) carboxylate complexes. *Journal of the American Chemical Society* 126(51):16692-16693.